Improvement of MRI-functional measurement with automatic movement correction in native and transplanted kidneys

Baudouin Denis de Senneville, Iosif Alexandru Mendichovszky, Sébastien Roujol, Isky Gordon, Chrit Moonen, Nicolas Grenier

Improvement of MRI-Functional measurement with automatic movement correction in native and transplanted kidneys

Baudouin Denis de Senneville, PhD[1,*], Iosif Alexandru Mendichovszky, PhD[2,*], Sébastien Roujol, M.Sc.[1,3], Isky Gordon, MD[2], Chrit Moonen, PhD[1], Nicolas Grenier, MD[1,4]

[1]: Laboratory for Molecular and Functional Imaging: From Physiology to Therapy, UMR 5231 CNRS/Université Bordeaux 2, 146 rue Léo Saignat, F - 33076 Bordeaux

[2]: UCL Institute of Child Health, 30 Guilford Street, London, WC1N 1EH

[3]: Ecole Nationale Supérieur d'Electronique, Informatique et Radiocommunications de Bordeaux, 1 avenue du docteur Albert Schweitzer, BP99, 33402 Talence

[4]: Service d'Imagerie Diagnostique et Interventionnelle de l'Adulte, Groupe Hospitalier Pellegrin, Place Amélie Raba-Léon - 33076 BORDEAUX Cedex

* Both authors have contributed equally

Address correspondence to:
Baudouin Denis de Senneville
Imagerie Moléculaire et Fonctionnelle, ERT CNRS
Université « Victor Segalen » Bordeaux 2
146 rue Leo Saignat, case 117
33076 Bordeaux, France

E-Mail: baudouin@imf.u-bordeaux2.fr
Tel: +33 5 57 57 45 93
Fax: +33 5 57 57 45 97

Grant support: European Union, NoE "Diagnostic Molecular Imaging"; Ligue National Contre le Cancer, Conseil Régional d'Aquitaine, Philips Medical Systems, CDTU canceropôle network, Kidney Research UK.

Running title: Kidney fMRI improvement with motion correction

ABSTRACT

Purpose: To improve 2D software for motion correction of renal dynamic contrast-enhanced magnetic resonance imaging (DCE-MRI) and to evaluate its effect using the Patlak-Rutland model.

Material and methods: A subpixel accurate method to correct for kidney motion during DCE-MRI was evaluated on native and transplanted kidneys using data from two different institutions with different magnets and protocols. The Patlak-Rutland model was used to calculate Glomerular Filtration Rate (GFR) on a voxel-by-voxel basis providing mean ($\overline{K}_p$) and uncertainty ($\overline{\sigma}(K_p)$) values for GFR.

Results: In transplanted kidneys, average absolute variation of $\overline{K}_p$ was 6.4 %±4.8 % (max= 16.6 %). In native kidneys average absolute variation of $\overline{K}_p$ was 12.11 % ±6.88 % (max= 25.6 %) for the right and 11.6 % ± 6 % (max= 20.8 %) for the left. Movement correction showed an average reduction of $\overline{\sigma}(K_p)$ of 6.9 %±6.6 % (max= 21.4 %) in transplanted kidneys, 30.9 %±17.6 % (max= 60.8 %) for the right native kidney and 31.8 %±14 % (max= 55.3 %) for the left kidney.

Conclusion: The movement correction algorithm showed improved uncertainty on GFR computation for both native and transplanted kidneys despite different spatial resolution from the different MRI systems and different levels of signal-to-noise ratios on DCE-MRI.

Key words: MRI-Functional measurement, kidney perfusion, glomerular filtration rate, movement correction

INTRODUCTION

Virtually all diseases of the kidney affect perfusion and glomerular filtration. Non-invasive and accurate measurement of both perfusion and glomerular filtration rate (GFR) could have a major impact in understanding renal physiopathology and for serial monitoring of the course of both acute and chronic kidney diseases. Dynamic contrast-enhanced (DCE) magnetic resonance imaging (MRI) is advocated to evaluate these functional parameters. However, publications in the literature show poor correlation when MRI-GFR has been compared with GFR measured by reference methods (1, 2); this poor correlation precludes the use of DCE-MRI for GFR estimation in daily clinical practice. The inaccuracy is multi-factorial with unsolved problems regarding the ideal acquisition sequence; the dual MR effect (T1 and T2*) of contrast agents; the conversion of signal intensity into concentration; the pharmacokinetic models applied, as well as the difficulties in post-processing (segmentation and region of interest). DCE-MRI images are usually acquired during spontaneous breathing that will result in kidney movement. Since respiratory-gated sequences (3) would lead to loss of temporal resolution, most groups studying DCE-MRI GFR have either repositioned images manually or ignored movement. However, movement causes artefacts in the pixel-based time-intensity analysis which will lead to inaccurate GFR quantification.

A compromise in choosing the acquisition parameters is required to achieve a sufficiently high signal-to-noise ratio (SNR). An ideal rapid isotropic 3D imaging of the moving kidneys is not achievable, and thus slices are usually oriented along the long axis of the kidney that will allow the best approximation of movement to be estimated. During DCE-MRI, voxel intensity changes may be due to one or more of the following factors: rapid, non-uniform movement of contrast within the different renal compartments; motion either due to respiration or physical

movement, or low SNR due to the MRI acquisition sequence required for rapid acquisition. Although movement can be addressed using image registration algorithms (4) applied in a post-processing step, this is not an option with the kidney as the image amplitude and contrast change with time due to the transit of the contrast agent through the kidney following a bolus injection (5).

The purpose of our study was to improve a 2D region tracking software for retrospective motion correction without sacrificing temporal resolution in quantitative renal DCE-MRI studies, code it into a radiologically useful software, and evaluate it using the Patlak-Rutland tracer kinetic model (6,7,8,9). This software was then applied to two different populations (healthy volunteers and renal transplant patients) in different institutions using different MRI scanners and different acquisition protocols. These protocols had different spatial resolutions and different levels of SNR. Motion during data acquisition may cause tracer kinetic model fitting errors in the post-processing step. Quantification of those model fitting errors may provide a quality criterion on motion correction and recent work demonstrated that it could even be used to drive the registration procedure (10). In this study, quantification of motion correction accuracy is based on tracer kinetic models. As this quantification depends heavily on the chosen model, we selected to evaluate the improvement after movement correction using the Patlak-Rutland model (see Appendix 1). Improvements in GFR shown with this registration algorithm might also apply when using other tracer kinetic models.

All computations were performed in 2D on the middle slice of each kidney.

MATERIALS AND METHODS

2D motion correction framework:

Theory

Let I_{ref} be the reference anatomical image and I_{cur} the current image to register. I_{ref} and I_{cur} are two 2D normalized greyscale images and the quantities $I_{ref}(x,y)$ and $I_{cur}(x,y)$ are the greyscale value of the two images at the coordinate (x,y) and the instant *t*. The objective was to relate the coordinate of each part of tissue in I_{cur} with the corresponding tissue in I_{ref}. A general definition for the problem of image registration can then be expressed as follow: registering $I_{ref}(x,y)$ and $I_{cur}(x,y)$ is equivalent to find a strategy to estimate a coordinate transformation *T* that maximizes:

$$\max_{T} \gamma\left(I_{ref}(x,y), I_{cur}\left(T(x,y)\right)\right) \qquad [1]$$

where γ is a criterion determining the accuracy of the registration. With image registration there is a compromise that has to be made between the complexity of the estimated spatial transformation *T* and the accuracy of the estimation strategy. Perturbations in image registration occur predominantly when the true motion field violates the brightness consistency model used for its approximation. In our case, because the contrast varies within the kidney with time, the algorithm has to be independent of the contrast changes within the kidney and also assumptions on the estimated kidney deformation have to be made. This work assumes that the kidney is a rigid body and its shape does not change during the MRI data acquisition. The new software takes into account that the two kidneys do not move equally with respiration and thus each kidney is dealt with separately during the correction process. Furthermore, the software has been developed to be virtually independent of operator interaction.

Proposed registration model

The implemented registration model was proposed by Sun et al (11). This approach, based on kidney edge invariance, was found to be the most promising technique for kidney registration during bolus passage (see Appendix 2). In its original form, the algorithm was based only on the estimate of translation displacements with a pixel resolution which might be insufficient for low amplitude movement as in transplants. Our implementation allows the estimation of a rigid transformation (translation + rotation) with subpixel accuracy.

Original DCE MR images were loaded into a home based registration software (implemented in C++). Only the kidneys and aorta are required for functional renal analysis, so image masking was performed, eliminating un-necessary anatomical structures. A region of interest (ROI) encompassing the renal parenchyma, excluding the renal sinus, was manually drawn by the radiologist on an enhanced image, taken during the vascular phase, when enhancement of the renal cortex is maximal. This image is the reference image set for motion estimation and is called image I_{ref}. Using this ROI, a binary mask (noted *m*) was constructed: pixels of the mask inside the kidney had a value of one, and outside a value of zero. Due to aliasing considerations, this mask was filtered with a 3×3 dilatation filter.

The 2D displacement of the kidney *T* was estimated by a 3 parameters rigid body model (2 translations + 1 rotation). Let $\theta_{ref}(x,y)$ and $M_{ref}(x,y)$ be the edge orientation and the edge magnitude for the pixel (x,y) obtained using a Sobel edge detector (12) on the reference image. Identically, let $\theta_{cur}(x,y)$ and $M_{cur}(x,y)$ be the edge orientation and the edge magnitude for the pixel (x,y) obtained on the current image to register. To the coordinate transformation *T* relating kidney motion, we used the edge-based consistency metric proposed by Sun et al. (11) as follow:

$$\gamma\left(I_{ref}(x,y), I_{cur}\left(T(x,y)\right)\right) = \frac{\sum_{x,y\in m} M_{ref}(x,y).M_{cur}\left(T(x,y)\right).\cos\left(2\left(\theta_{ref}(x,y) - \theta_{cur}\left(T(x,y)\right)\right)\right)}{\sum_{x,y\in m} M_{ref}(x,y).M_{cur}\left(T(x,y)\right)} \qquad [2]$$

An exhaustive search was performed to determine parameters of T that maximises γ. A multi-step scheme was used to perform a subpixel registration while reducing enumeration of possible solutions. First, all possible values for the three parameters of T were explored with an accuracy of one pixel for translation and one degree of accuracy for rotation. Respiratory displacement of the kidney is mainly a cranio-caudal shift. Based on preliminary observations, the size of the search space was restrained to values of 31 pixels for cranio-caudal direction, 11 pixels for left-to-right direction and 5 degrees for in-plane rotations (these typical values were defined with respect to maximal kidney amplitude and image resolution in our data). Following this, an exhaustive search was performed with a step of 0.25 pixels for translation parameters to further enhance the accuracy of the registration to a sub-pixel level. The grey level intensity of pixels of the registered image was computed with a bilinear interpolation from the original brightness values. The ROI could then be propagated to all images of the time series.

If the motion had been accurately corrected, the kidney border would coincide with the contour of the original kidney ROI. An experienced operator reviewed the re-aligned data set and made manual small adjustements, based on a visual analysis, in case of small misalignements. When the realignment was visually considered as impossible because of intra-scan or excessive out-of-plane movements, the image was rejected. The corrected images were exported back into their native format and loaded into a dedicated software package MIStar (Apollo Medical Imaging, Melbourne, Australia) for processing using the Patlak-Rutland model.

Patients

The movement correction algorithm was tested on DCE-MRI renal studies obtained in 2 different populations: 10 patients following kidney transplantation (age ranging from 24 to 63 years, mean 45) with variable renal function (creatinine clearance between 17 and 59.4 ml/min,

mean 44.15 ml/min); and 10 healthy volunteers (age ranging from 23 to 36 years, mean 29.2). Both studies received approval from the local ethics committees and all participants gave written informed consent for taking part in the studies.

MR acquisition protocol:

Following kidney transplantation, the patients underwent the MRI examination on a 1.5 T Philips system (ACS-NT, Philips Medical System, Best, The Netherlands) using a body phased-array coil and a 3D SR-TFE pulse sequence, without fat saturation, with the following parameters: TR = 4.4 ms, TE = 2.5 ms, TI = 120 ms, FOV = 400×400 mm², FA = 10°, resulting in a temporal resolution of 1.5 seconds (per kidney volume). To ensure complete coverage of the kidney 5 slices (10 mm thick, no gap) were acquired for each dynamic volume, with an in-plane resolution of 128×50 pixels and a resulting voxel size of 3.2×8×10 mm^3. During the functional scan a dose of 0.03 mmol (0.06 ml/kg) of Gd-DOTA (Dotarem®, Guerbet Group, Aulnay-sous-Bois, France) was injected, followed by a 20 ml flush of saline, both with a 2ml/sec injection rate, using an automatic injector (MedRad). This acquisition contained a total of 200 dynamic volumes over a total time of 300 seconds.

The healthy volunteers were scanned on a 1.5 T Siemens scanner (Avanto, Siemens Medical Solutions, Erlangen, Germany) with a dedicated abdominal TIM coil. The dynamic contrast-enhanced acquisition was performed using a gradient-echo 3D-FLASH pulse-sequence (VIBE) with the following parameters: TR = 1.63 ms, TE = 0.53 ms, flip angle = 17, strong fat saturation, PAT factor = 2 (GRAPPA), FOV = 400×325 mm², 18 slices covering the entire kidney, 7.5 mm slice thickness, no gap. The resulting voxel size was 3.1×3.1×7.5 mm^3 and each dynamic volume was acquired every 2.5 seconds. A 0.05 mmol (0.1 ml) /kg body weight dose of Gd-DTPA (Magnevist, Schering, Germany) was injected as a bolus at 2 ml/second injection rate

using an automatic injector (Spectris). The contrast agent bolus was immediately followed by a 15 ml saline flush injected at the same speed. A total of 138 volumes were acquired in 345 seconds.

During the scans both patients and volunteers were asked to breathe normally and lie relaxed in the scanner. In both groups the slices were positioned in an oblique-coronal plane (along the long axis of the kidney) to minimise through-plane movement and ensure the presence of the aorta on at least one slice, needed for subsequent analysis using the Patlak-Rutland model (see Appendix 1).

Assessment of Movement Correction:

A manual ROI was generated for the cortex of each kidney on both sets of images. This ROI was different from the one used for movement correction and was drawn on the early enhanced image I_{ref}. The arterial input function (AIF), required for the Patlak-Rutland analysis, was obtained from a manual ROI drawn on the aorta (volunteers) or iliac artery (transplant patients), just above the renal artery. The influence of inflow effects was minimised by the oblique-coronal positioning of the slices during data acquisition and no sign of inflow effects was observed during the Patlak analysis. For an objective in-vivo evaluation of the algorithm, we estimated single kidney GFR on the corrected and non-corrected data. Numerous publications have used the Patlak-Rutland model for estimation of the glomerular filtration of the cortex and or kidney (6,7,8,9). GFR was calculated using this model on a voxel-by-voxel basis providing two 2D functional GFR maps with GFR values (noted K_p) within the cortex, and a standard deviation map (noted $\sigma(K_p)$). $\sigma(K_p)$ relates the uncertainty on GFR computation and was thus used as a quality criterion in our study. For each kidney a mean of K_p (noted $\overline{K}_p$) and a mean of

σ(K_p) (noted $\bar{\sigma}(K_p)$) over the cortical ROI were calculated using the time period of 60 – 120 seconds post Gd contrast injection, considering time zero the first rise (more than 2 standard deviations) of the AIF signal from the baseline.

These results were then compared between the uncorrected and movement corrected data. As a number of questions relating to accurate GFR computation still remain unanswered (how to accurately evaluate kidney volumes? do transplant and native kidneys function identically as far as perfusion and filtration are concerned?), only relative variations of K_p and $\bar{\sigma}(K_p)$ were analysed.

Statistics

$\bar{\sigma}(K_p)$ values from uncorrected and movement corrected data were compared using a Student t-test, considering as significant a p-value < 0.05.

RESULTS

Computation time on an Athlon 3.2 Ghz with 1.5 GB of RAM to correct a masked image series was 15 and 7 minutes for native and transplanted kidneys, respectively.

Visual assessment of the movement corrected data showed that manual repositioning was rarely required (in less than 1 % of all images in both groups) and few images were considered as too corrupted and rejected (less than 1 % of all images in both groups were rejected). Only a few seconds were thus necessary for this manual step.

Patients with renal transplants

The typical amplitude of estimated renal displacement of transplanted kidneys didn't exceed one pixel, clearly indicating the importance of sub-pixel accuracy in the registration process.

Fluctuations in signal intensity time-curves, averaged over the cortical ROI were reduced in all cases following movement correction (illustrated in Figure 1). This is also reflected in the reduced dispersion of data on the Patlak-Rutland plot as shown in Figure 2. Figure 3 illustrates the 2D GFR and standard deviation maps before and after motion correction for the same patient. $\overline{K}_p$ and $\overline{\sigma}(K_p)$ values for each patient before and after motion correction are presented in Figure 4. The average absolute variation of $\overline{K}_p$ for the entire group was 6.4 % ± 4.8 % (max = 16.6 %). There was a significant reduction of $\overline{\sigma}(K_p)$ on motion corrected data sets (p = 0.003 Student t-test) compared to the non-corrected ones, with an average reduction of $\overline{\sigma}(K_p)$ of 6.9 % ± 6.6 %. One patient (number 4) had a $\sigma(K_p)$ of 21.4 % as shown on Figure 2.

Healthy volunteers with native kidneys

Right and left kidneys have been analyzed individually. Before motion correction, mean amplitude of estimated renal displacement of native kidneys was 6 pixels on the right side and 8 pixels on the left side. Figure 5 illustrates an example of the 2D GFR and standard deviation maps before and after motion correction. $\overline{K}_p$ and $\overline{\sigma}(K_p)$ values for each volunteer before and after motion correction are presented in Figure 6. The average absolute variation of $\overline{K}_p$ for the right kidney was 12.11 % ± 6.88 % (max = 25.6 %), and 11.6 % ± 6 % (max = 20.8 %) for the left kidney. A significant reduction of $\overline{\sigma}(K_p)$ values was obtained on motion corrected data sets, with p = 0.003 (right kidney) and p = 0.002 left kidney (Student t-test). The average reduction of

$\bar{\sigma}(K_p)$ was 30.9 % ± 17.6 % (max = 60.8 % for patient number 4) for the right kidney, and 31.8 % ± 14 % (max = 55.3 % for patient number 1) for the left kidney.

DISCUSSION

The clinical use of DCE-MRI in renal studies has led to publications on quantification of the MR signal for both perfusion and GFR. None of the publications to date have applied any motion correction algorithm routinely to the data, yet this variable must be taken into account for any accurate quantification. Furthermore, there is no published evaluation of the accuracy of an automatic movement correction method applied to renal DCE-MRI. The registration method used in this study is based on the one proposed by Sun et al (11). To increase the accuracy, our algorithm estimates a rigid body transformation with subpixel accuracy. Changes in signal intensity due to bolus passage within the kidney do not affect the efficiency of our approach. Visual assessment of the movement corrected data showed little movement in more than 98 % of tested data sets.

Accuracy of image registration algorithms can easily be quantified on synthetic or phantom data as the motion is fully controlled. However, actual organ displacement in-vivo is unknown. The approach whereby comparisons are made between corrected data using a post-processing algorithm versus manual correction by several operators is questionable. Furthermore, using several operators as a reference method introduces important uncontrollable variables that reduce reproducibility. This study has used an established tracer kinetic model (Patlak-Rutland model) which is independent of the user. The data following movement correction showed a reduced standard deviation with improvement of GFR uncertainty (up to 21.4 % reduction on

GFR uncertainty in transplanted kidneys and 60.8 % in native kidneys). The mean of $\overline{K}_p$ and $\overline{\sigma}(K_p)$ variations for the transplant group are low (resp. 6.4 % and 6.9 %) compared to the standard deviation (resp. ± 4.8 % and ± 6.6 %). This relates to a wide dispersion of values around the mean (maximum resp. 16.6 % and 21.4 %) due to the different degrees of movement from one patient to another. Therefore, while a variation of less than 5 % was obtained in 4 patients for $\overline{K}_p$ and in 5 patients for $\overline{\sigma}(K_p)$, a significant variation (greater than 10 %) was obtained on 2 patients for $\overline{K}_p$ values and 3 patients for $\overline{\sigma}(K_p)$ values. In the native kidney group, $\overline{K}_p$ variation > 5 % was obtained in 7 volunteers on the right kidney and in 9 volunteers on the left kidney; also a $\overline{\sigma}(K_p)$ variation > 10 % was obtained in 9 volunteers on the right and in all volunteers on the left. These results suggest that motion correction is a necessary pre-requisite for quantification of DCE renal MRI in all cases.

Full analysis of the displacement of the kidneys requires a 3D image registration. The ideal image plane of renal DCE-MRI is along the long axis of the kidney which is the main axis of respiratory movement. The importance of a 3D correction algorithm can not be assessed from this study, but as the majority of the movement is along the long axis of the kidney, one may suggest that its added value might be small. As the transplant kidney lies at some distance from the diaphragm, movement correction in this clinical situation becomes less critical. This is reenforced by the results of this study where the improvement of GFR uncertainty is much smaller in the transplant group than in the normal volunteers. However, in transplanted kidneys number 3 and 9 some residual motion outside the imaging plane could explain why the motion correction didn't show improvement of GFR uncertainty (see Figure 4b).

Comparison with other existing approaches for kidney registration

Althought navigator echoes can be used to estimate kidney displacement (13), motion information is in this case restricted to translational motion in the direction of the navigator. Alternatively, kidney displacement can be estimated on MR images using image registration algorithms and three main classes of approaches can be distinguished in the literature (details for each approach are given in Appendix 2):

1) methods based on grey level intensity conservation,
2) Fourier based approaches,
3) methods based on geometrical characteristics invariance.

Methods based on grey levels intensity conservation and Fourier-based approaches are both very sensitive to the determination of the mask size in which the registration is computed. An extension of this mask allows inclusion of surrounding anatomical structures to the registration process. Tissues closely surrounding the kidneys are not affected by bolus passage that may help the registration process, further efficiency of the registration process occurs by restraining computation to the desired part of the image. A delicate compromise must thus be found for the mask size in each patient study and each MR acquisition sequence. Critically, these two approaches are both sensitive to voxel intensity variation. This is a major drawback as the signal within the kidney changes significantly with time over the critical period required for analysis (due to the passage of the contrast agent through the kidney). Thus the change in voxel intensity may be due either to renal movement or to the normal passage of contrast within the kidney. This adds to the difficulty of absolute movement estimation (one identical image is always used as the reference image for the registration of the time series). Although these approaches to image registration can be sufficient in some cases (when contribution of contrast modification induced by the bolus is small compared to contribution of surrounding anatomical

structures, as, for example, when no fat suppression is performed during the MR acquisition procedure), incremental estimation (14) is generally required (the displacement of the kidney is determined between subsequent images, the first image of each pair being the reference image). For each image, a visual verification is required by the user and manual adjustment of the location of the mask with respect to the kidney is performed when needed. Automatic movement correction requires a more robust approach.

Contrary to the two previously mentioned approaches, methods based on geometrical characteristics invariance are fully stable with respect to the dynamic movement of the contrast agent through anatomical structures (15). This approach overcomes the problems related to voxel intensity variation during DCE-MRI acquisition and kidney motion estimation is not affected by the passage of contrast agents. Therefore, absolute motion estimation is feasible, allowing reduction in operator errors (especially for transplanted kidneys) and reduction in processing time required for movement correction by the radiologist. Limiting the mask size helps in restraining possible interferences generated by surrounding anatomical structures (induced, for example, by possible displacement outside the imaging plane) and increasing registration accuracy by limiting the computation to the desired part of the image.

No movement correction algorithm is perfect for DCE-MRI studies and the drawbacks of these techniques are their sensitivity to noise, change in kidney shape during acquisition or magnetic field homogeneity changes. Low SNR values in the renal parenchyma were only observed for dynamics acquired before bolus injection when using strong fat suppression in the volunteer MR protocol. Therefore, noise sensitivity does not represent a major limitation. Changes in kidney shape during MR acquisition occur when motion outside the imaging plane and/or intra-scan motion artefacts are present. Such images are usually severely degraded and are removed from the analysis process. In this study, with 2 different MR acquisition protocols, this

phenomenon occurred in less than 1 % of the total acquired images. Changes in magnetic field homogeneity at different time points in the respiratory cycle are difficult to correct and were not addressed in our study. Such changes may also lead to image distortion (in particular with long EPI acquisition train lengths).

In conclusion, the implemented registration method appeared to be efficient for movement correction for DCE-MRI in both native and transplanted kidneys. The correction method was independent of the MR acquisition parameters (SNR, spatial resolution, fat suppression) and operator intervention. Motion correction is a necessary pre-requisite to improve quantification of renal functional parameters. The results showed that the correction of native kidney displacements allowed a significant uncertainty reduction on the computed GFR with the Patlak-Rutland plot technique. However, the gain is modest in pelvic renal transplants due to low displacement amplitude. Other limiting factors such as the linearity of the signal with gadolinium concentration, the cortical volume measurement, and an accurate ROI positioning have to be solved. Then, a quantification of the error reduction in GFR measurement could be performed in future using a reference method and applied to a population with a large range of GFR values. Although registration has been tested in 2D, all observations will be tested in the 3D case when technological progress in rapid MR acquisition sequence will allow sufficient spatial and temporal resolution.

APPENDIX 1: Patlak-Rutland model

The Patlak-Rutland plot technique describes a two compartment model with unilateral tracer flow from compartment 1 (the vascular space) into compartment 2 (nephron space) (6,7,8,9). The following assumptions are made:

- The interstitial space as a third space is neglected.
- Signal change is proportional to the concentration of gadolinium in a voxel.
- Prompt and complete gadolinium mixes inside the compartments.
- Hematocrit is constant in all renal vessels and the aorta.
- The gadolinium concentration in the aorta and the renal arteries is equal at any time.

The amount of gadolinium in the renal parenchyma *R(t)* can be expressed as the sum of gadolinium in the vascular space *B(t)* and the nephron *Q(t)* :

$$R(t) = B(t) + Q(t) \qquad [3]$$

Two assumptions are then made:

- The amount of gadolinium the vascular space *B(t)* is proportional to the concentration of gadolinium in the aorta *b(t)*.
- The amount of gadolinium filtered into the nephron is proportional to the integral of the gadolinium concentration curve of the aorta.

Those two assumptions can be mathematically expressed as follow:

$$\begin{cases} B(t) = c_1 . b(t) \\ Q(t_1) = c_2 . \int_0^t b(x)\,dx \end{cases} \qquad [4]$$

c_2 is equivalent to the gadolinium clearance from the vascular space into the nephron. The combination of equations [3] and [4] leads to:

$$R(t) = c_1.b(t) + c_2.\int_0^t b(x)\,dx \qquad [5]$$

When equation [5] is divided by *b(t)*, the Patlak-Rutland plot equation is obtained :

$$\frac{R(t)}{b(t)} = c_1 + c_2.\frac{\int_0^t b(x)\,dx}{b(t)} \qquad [6]$$

Equation [6] is computed for each dynamics in the 60-120 seconds time frame. The obtained plot leads to a straight line with a slope (c_2) equal to the GFR (see figure 2). c_2 is then determined using a least square fit. Computation of c_2 is performed for each voxel of the renal parenchyma to obtain a 2D GFR map (noted K_p). Quality maps (noted $\sigma(K_p)$) are then obtained by computing, for each voxel, the standard deviation of the differences between measured and fitted values. A mean of K_p (noted $\overline{K}_p$) and of $\sigma(K_p)$ (noted $\overline{\sigma}(K_p)$) over the cortex can then be calculated.

APPENDIX 2: Existing approaches for kidney registration

Three main classes of approaches for kidney tracking during bolus passage have been observed in the literature:

Methods based on grey levels intensity conservation

Those methods assume that *M* in equation [1] is a similarity criterion, computed on grey levels intensities, between the part of a reference image containing the kidney and the area it overlays in the image to register (14,16). A number of similarity criteria have been proposed in the literature (4). High order criteria are robust to noise but, as a counterpart, are more sensitive to grey level intensities modification induced by the bolus. Inter-correlation coefficient is

generally used as it offers the best compromise for kidney registration during perfusion (16). The objective is then to find parameters of the parametric spatial transformation that optimize this similarity criterion. For that purpose, exhaustive search or gradient driven approach are generally used.

Fourier based approaches

Those methods aim to express datasets in a new domain of representation and to exploit the new domain proprieties to estimate motion. For example, registration problems involving pure translation can be recovered by computing a phase difference in Fourier domain (14). Methods have been proposed to allow sub-pixel accuracy (17), and estimation of more complex displacements (a log-polar transformation is applied to the magnitude spectrum and the rotation and scale is recovered by computing phase difference in the log-polar space (18,19)). Fourier-based approaches are very low time consuming and also more robust to estimate translation motion than methods based on grey levels intensity (see (14)).

Methods based on geometrical characteristics invariance

Several template matching approaches based on geometrical characteristics invariance have been proposed in the literature. Gerig et al. have developed in 1991 a template matching between an estimated contour of the kidney and a manually drawn contour model (20). A linear transformation (rotation plus translation) was chosen to estimate the displacement between the two contours, and a bicubic interpolation was used for ensuring sub-pixel accuracy. The more recent and the most interesting method based on geometrical characteristics invariance has been proposed by Sun et al (11). The principle is the following: although the relative intensities between tissues vary with time, edges orientation along tissue boundary is always parallel across

the image sequence. Note that, in its proposed form, the registration algorithm is combined with an auxiliary image segmentation step which is not evaluated in the current paper.

REFERENCES

(1) Buckley DL, Shurrab AE, Cheung CM, et al. Measurement of single kidney function using dynamic contrast-enhanced MRI: comparison of two models in human subjects. J Magn Reson Imaging 2006:24:1117-23.

(2) Lee VS, Ruzinek H, Bokacheva L, et al. Renal function measurements from MR renography and a simplified multicompartmental model. Am J Physiol Renal Physiol. 2007:292:F1548-59

(3) Moricawa S, Inubushi T, Kurumi Y, Naka S, Seshan V, Tsukamoto T. Feasibility of simple respiratory triggering in mr-guided interventional procedures for liver tumors under general anesthesia. In: Proceedings of the 10th Annual Meeting of ISMRM, Hawaii, 2002.

(4) Maintz JBA, Viergever MA, A survey of medical image registration, Medical Image Analysis, 1998:2(1):1-36.

(5) Yim PJ, Marcos HB, McAuliffe M, McGarry D, Heaton I, Choyke PL, Registration of time series Gd-contrast enhanced magnetic resonance images for renography, in Proc. 14th IEEE Symp. Computer-Based Medical Systems, pp.516-520, 2001.

(6) Patlak CS, Blasberg RG, Fenstermacher JD, Graphical evaluation of blood-to-brain transfer constants from multiple-time uptake data. J Cereb Blood Flow Metab. 1983;3(1):1-7.

(7) Rutland MD, A single injection technique for subtraction of blood background in ^{131}I-hippuran renograms. Br J Radiol. 1979;52(614):134-7.

(8) Hackstein N, Heckrodt J, Rau WS, Measurement of single-kidney glomerular filtration rate using a contrast-enhanced dynamic gradient-echo sequence and the Rutland-Patlak plot technique, JMRI, 18:714-725, 2003.

(9) Annet L, Hermoye L, Peeters F, Jamar F, Dehoux JP, Van Beers BE, Glomerular Filtration Rate: Assessment with dynamic contrast-enhanced MRI and a cortical compartment model in the rabbit kidney, JMRI, 20:843-849, 2004.

(10) Buonaccorsi G, Roberts C, Cheung S, et al. Comparison of the Performance of Tracer Kinetic Model-Driven Registration for Dynamic Contrast Enhanced MRI Using Different Models of Contrast Enhancement. Academic Radiology, Volume 13, Issue 9, Pages 1112-1123.

(11) Sun Y, Jolly MP, Moura JMF, Integrated registration of dynamic renal perfusion MR images, In: Proceedings of IEEE International Conference on Image Processing, Singapore, 2004:3:1923-1926.

(12) Gonzalez RC, Woods RE, Digital Image Processing, In: Prentice Hall editor, Second Edition, 2001:p 578-579.

(13) de Zwart J. A., Vimeux F. C., Palussière J., Salomir R., Quesson B., Delalande C., et al. On-line correction and visualization of motion during MRI-controlled hyperthermia, Magnetic Resonance in Medicine, 2001;45(1):128-37.

(14) Giele ELW, de Priester JA, Blom JA, et al. Movement correction of the kidney in dynamic MRI scans using FFT phase difference movement detection, Journal of Magnetic Resonance Imaging, 2001:14: 741-749.

(15) Yim PJ, Marcos HB, McAuliffe M, McGarry D, Heaton I, Choyke PL, Registration of time-series contrast enhanced magnetic resonance images for renography, In: Proceedings of the 14th IEEE Symposium on Computer-Based Medical Systems, 2001:516–520.

(16) Gupta SN, Solaiyappan M, Beache GM, Arai AE, Foo TK, Fast method for correcting image misregistration due to organ motion in time-series MRI data, Magn Reson Med, 2003:49(3):506-514.

(17) Shekarforoush H, Berthod M, Zerubia J, Subpixel image registration by estimating the polyphase decomposition of cross power spectrum. In: proceedings of the IEEE Computer Society Conference on Computer Vision and Pattern Recognition, USA, 1996:532-537.

(18) Reddy BS, Chatterji BN, An fft-based technique for translation, rotation, and scale-invariant image registration, IEEE Trans. Pattern Analyses and Machine Intelligence, 1996:5(8):1266-1270.

(19) Wolberg G, Zokai S, Robust Image Registration Using Log-Polar Transform, In: Proceedings of IEEE International Conference on Image Processing, Vancouver, 2000.

(20) Gerig G, Kikinis R, Kuoni W, von Schulthess GK, Kubler O, Semiautomated ROI analysis in dynamic MR studies. Part I: Image analysis tools for automatic correction of organ displacements, J Comput Assist Tomogr, 1991:15:725-732.

FIGURE LEGENDS

Figure 1. Example of time intensity attenuation curves obtained on a kidney following a renal transplantation. The temporal evolution of the mean MR signal intensity over the cortical ROI (*R(t)* in arbitrary units) is reported without (**b**) and with (**c**) the applied motion correction. Note the decrease of fluctuations in signal intensity time curves after movement correction.

Figure 2. Example of Patlak-Rutland plots obtained on a transplanted kidney without (**a**) and with the applied motion correction (**b**) (results are reported in arbitrary units for each axis as relative changes in computed GFR with movement correction in this study). Note that, kidney motion correction allows here 21.4 % of average reduction of the standard deviation in the Patlak-Rutland plot ($\overline{\sigma}(K_p)$).

Figure 3. Example of 2D GFR (**a,b**) and standard deviation (**c,d**) maps on transplanted kidney reported in Fig. 1a (results are reported as relative changes in computed GFR with movement correction in this study), without (**a,c),** and with (**b,d)** motion correction. Standard deviation values are lower and more homogeneously distributed with (**d**), than without (**c**) motion correction.

Figure 4. Performances comparison between uncorrected and corrected data sets on the 10 patients with kidney transplants, **a:** variation of computed GFR ($\overline{K}_p$). **b:** improvement GFR uncertainty ($\overline{\sigma}(K_p)$). Movement correction shows an average absolute variation of $\overline{K}_p$ of 6.4 %±4.8 % (max= 16.6 %) and an average reduction of $\overline{\sigma}(K_p)$ of 6.9 %±6.6 % (max= 21.4 %).

Figure 5. Example of 2D GFR (**b,c**) and standard deviation (**d,e**) maps obtained on native kidneys reported in (**a**) (arbitrary units), without (**b,d),** and with (**c,e)** motion correction. Standard deviation values are lower and more homogeneously distributed with (**e**), than without (**d**) motion correction.

Figure 6. Performances comparison between uncorrected and corrected data sets on right (**a,b**) and left (**c,d**) kidneys for 10 healthy volunteers. **a,c:** percentage of averaged GFR variation ($\overline{K}_p$). **b,d:** improvement of GFR uncertainty ($\overline{\sigma}(K_p)$). Movement correction shows an average absolute variation of $\overline{K}_p$ of 12.11 % ±6.88 % (max= 25.6 %) for the right kidney and 11.6 % ± 6 % (max= 20.8 %) for the left. The average reduction of $\overline{\sigma}(K_p)$ was 30.9 %±17.6 % (max= 60.8 %) for the right kidney and 31.8 %±14 % (max= 55.3 %) for the left.

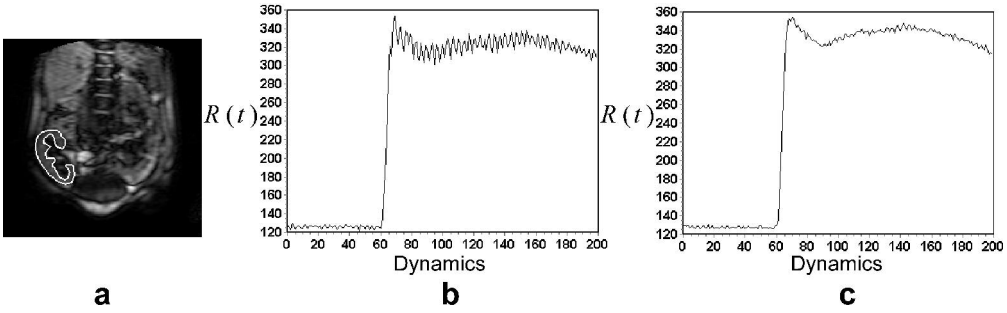

Figure 1. Example of time intensity attenuation curves obtained on a kidney following a renal transplantation. The temporal evolution of the mean MR signal intensity over the cortical ROI (*R(t)* in arbitrary units) is reported without (b) and with (c) the applied motion correction. Note the decrease of fluctuations in signal intensity time curves after movement correction.

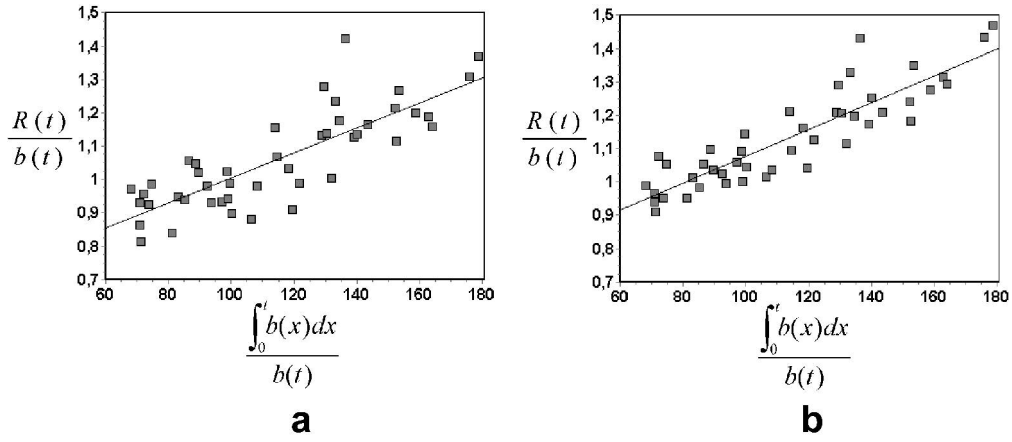

Figure 2. Example of Patlak-Rutland plots obtained on a transplanted kidney without (a) and with the applied motion correction (b) (results are reported in arbitrary units as relative changes in computed GFR with movement correction in this study). Note that, kidney motion correction allows here 21.4 % of average reduction of the standard deviation in the Patlak-Rutland plot (mean of σ (K_p)).

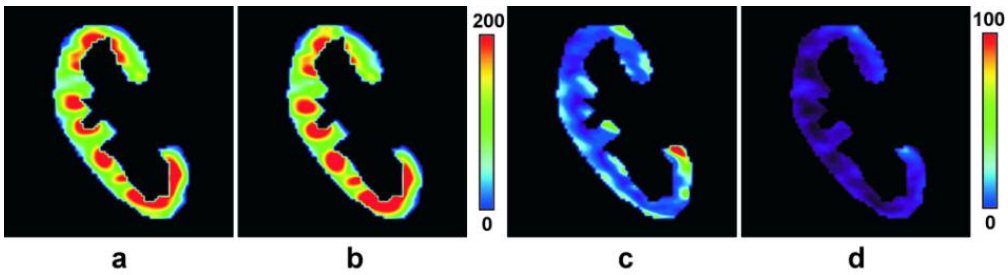

Figure 3. Example of 2D GFR (a, b) and standard deviation (c, d) maps on transplanted kidney reported in Fig. 1a (results are reported as relative changes in computed GFR with movement correction in this study), without (a,c), and with (b,d) motion correction. Standard deviation values are lower and more homogeneously distributed with (d), than without (c) motion correction.
80x21mm (300 x 300 DPI)

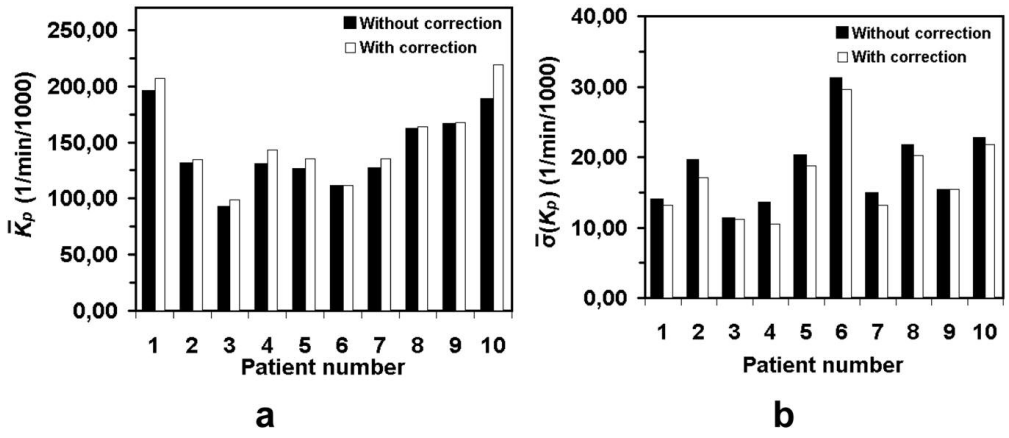

Figure 4. Performances comparison between uncorrected and corrected data sets on the 10 patients with kidney transplants, a: variation of computed GFR (mean of K_p), b: improvement GFR uncertainty (mean of $\sigma(K_p)$). Movement correction shows an average absolute variation of computed GFR of 6.4 %±4.8 % (max= 16.6 %) and an average reduction of GFR uncertainty of 6.9 %±6.6 % (max= 21.4 %).
57x24mm (600 x 600 DPI)

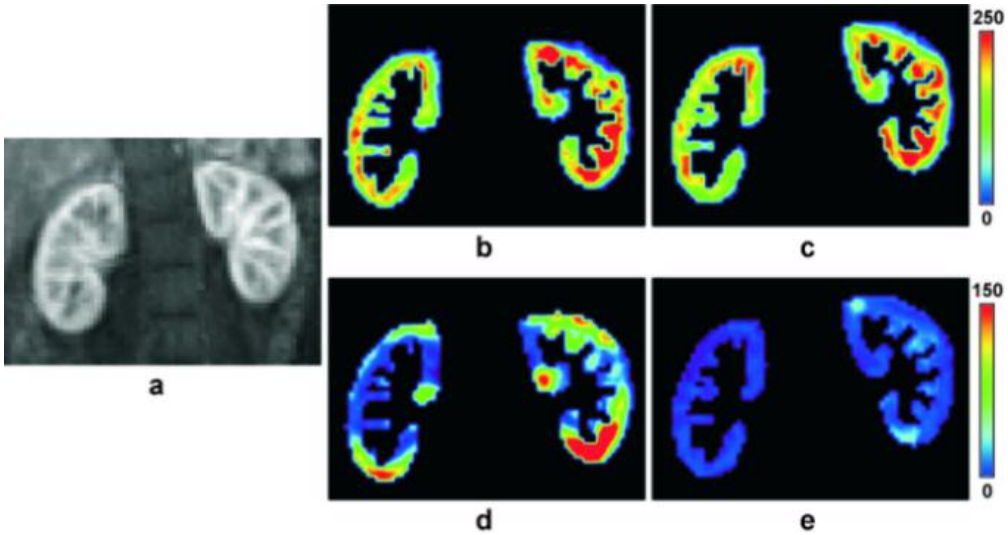

Figure 5. Example of 2D GFR (b, c) and standard deviation (d, e) maps obtained on native kidneys reported in (a) (arbitrary units), without (b,d), and with (c,e) motion correction. Standard deviation values are lower and more homogeneously distributed with (e), than without (d) motion correction.
57x30mm (300 x 300 DPI)

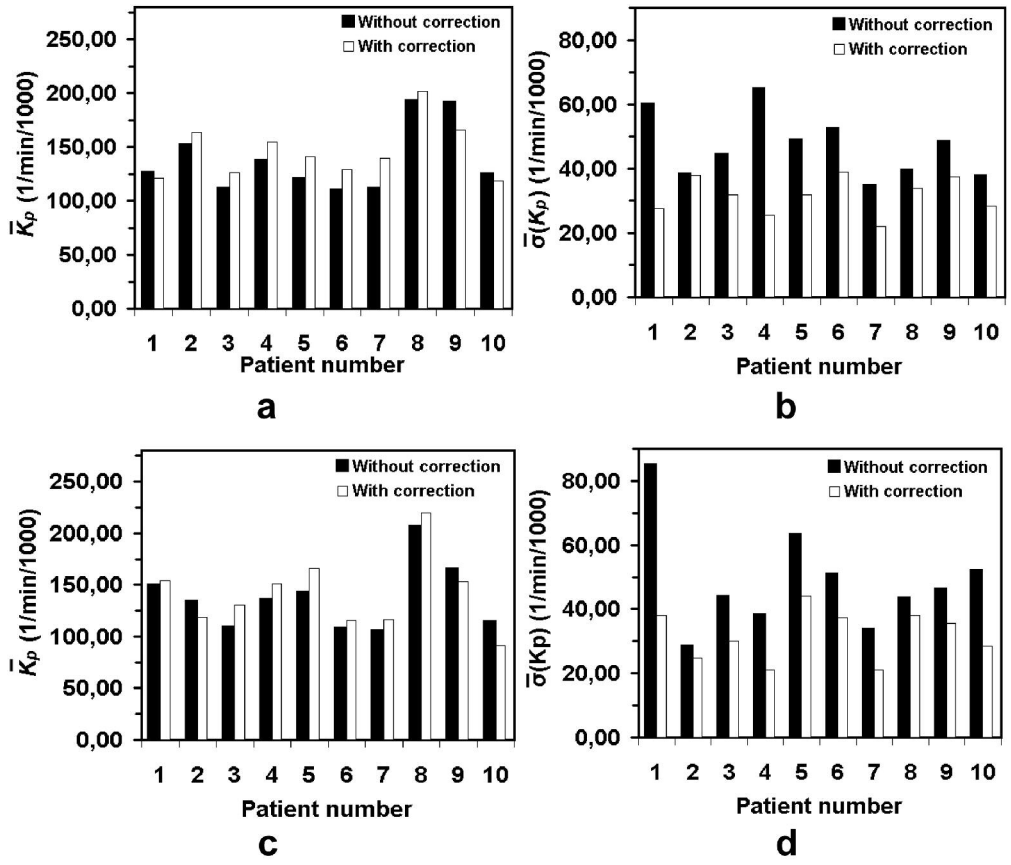

Figure 6. Performances comparison between uncorrected and corrected data sets on right (a, b) and left (c, d) kidneys for 10 healthy volunteers. a,c: percentage of averaged GFR variation (mean of K_p). b,d: improvement of GFR uncertainty (mean of $\sigma(K_p)$). Movement correction shows an average absolute variation of GFR variation of 12.11 % ±6.88 % (max= 25.6 %) for the right kidney and 11.6 % ± 6 % (max= 20.8 %) for the left. The average reduction of GFR uncertainty was 30.9 %±17.6 % (max= 60.8 %) for the right kidney and 31.8 %±14 % (max= 55.3 %) for the left.

114x98mm (600 x 600 DPI)